

Assessment of the $k - \epsilon$ Turbulence Model for Compressible flows using Direct Simulation Data

Krishnendu Sinha*

Aerospace Engineering and Mechanics
Army High Performance Computing Research Center
University of Minnesota, Minneapolis, MN 55455

M. Pino Martín†

CTR/NASA Ames Research Center
Moffett Field, CA 94035

Graham V. Candler‡

University of Minnesota

Abstract

We evaluate the $k - \epsilon$ turbulence model using direct numerical simulation (DNS) data of a Mach 4 boundary layer. We find that the low Reynolds number damping functions for the Reynolds stress must be corrected by the density ratio to match the DNS data. We present the budget of the k equation and assess the modeling of the various source terms. The models for all the source terms, except for the production and dilatational dissipation terms, are found to be adequate. Finally, we present the solenoidal dissipation rate equation and compute its budget using the boundary layer data. We compare this equation with the dissipation rate equation in an incompressible flow to show the equivalence between the two equations. This is the basis for modeling the solenoidal dissipation equation. However, an additional term in the equation due to variation of fluid viscosity needs to be modeled.

1. Introduction

The $k - \epsilon$ turbulence model is widely used to simulate incompressible and compressible flows. In this model, transport equations for the turbulent kinetic energy, k , and its dissipation rate, ϵ , are solved. The Reynolds stress is then modeled in terms of k and ϵ , along with a damping function to account

for the low Reynolds number, Re , effects close to a solid wall. The modeling of the unclosed terms in k and ϵ equations, and the low Re damping function are mostly based on dimensional arguments. The validity of these assumptions often limit the performance of the model when applied to engineering problems. The $k - \epsilon$ turbulence model has been tested against a wide range of experimental data. However, most of the data are limited to the mean flow quantities. The higher order correlations involved in the unclosed terms are difficult to measure experimentally. By comparing the model prediction of the mean flow quantities with the experimental data, one can assess the overall performance of the turbulence model but cannot evaluate the assumptions made for each unclosed term. In this regard, a direct numerical simulation (DNS) database is very useful, wherein the unclosed terms can be evaluated exactly and compared to their modeled counterpart.

DNS of simple flows have been previously used to develop and test turbulence models. However, most of the work has been done for incompressible flows. Mansour *et al.*¹ used DNS data of channel flows to compute the budget of the Reynolds stresses and the dissipation rate of the turbulent kinetic energy. The existing closure models for the source terms were tested against the DNS data and were found to be inadequate. Rodi and Mansour² evaluated various low Re damping functions against DNS data of channel and boundary layer flows. They also tested existing models for the ϵ -equation and proposed new models based on the DNS data. Also, Nagano and Shimada³ presented comprehensive DNS-based modeling for the Reynolds stress, and the source terms in the k and ϵ equations. The latest work in this direction is by Sarkar and So⁴

*Graduate Research Assistant, Student Member AIAA

†Research Associate, Member AIAA

‡Professor, Senior Member AIAA

Copyright © 2001 by Krishnendu Sinha. Published by the American Institute of Aeronautics and Astronautics, Inc. with permission.

Model	Code	D	f_μ
Launder-Sharma	LS	$2\nu\sqrt{k}_{,y}^2$	$\exp(-3.4/(1 + 0.002Re_T)^2)$
Chien	CH	$2\nu k/y^2$	$1 - \exp(-0.0115y^+)$
Lam-Bremhorst	LB	0	$[1 - \exp(-0.0165y^*)]^2 (1 + 20.5/Re_T)$
Shih-Mansour	SM	$2\nu\sqrt{k}_{,y}^2$	$1 - \exp(-6 \times 10^{-3}y^+ - 4 \times 10^{-4}y^{+2} + 2.5 \times 10^{-6}y^{+3} - 4 \times 10^{-9}y^{+4})$
Nagano-Tagawa	NT	0	$[1 - \exp(-y^+/26)]^2 (1 + 4.1/Re_T^{3/4})$
Rodi-Mansour	RM	$2\nu\sqrt{k}_{,y}^2$	$1 - \exp(-2 \times 10^{-4}y^+ - 6.5 \times 10^{-4}y^{+2})$
Myong-Kasagi	MK	0	$(1 + 3.45/\sqrt{Re_T}) [1 - \exp(-y^+/70)]$

Table 1. Damping function, f_μ , used in different low Re versions of the $k - \epsilon$ turbulence model. Here, $y^+ = u_\tau y/\nu_w$, $y^* = k^{1/2}y/\nu_w$ and $Re_T = k^2/\nu\epsilon$.

where DNS data for complex flows is used for evaluating models.

DNS based modeling for compressible flows is more limited than for incompressible flows. The transport equation for the turbulent kinetic energy in a compressible flow is similar to the incompressible equation, but has additional source terms due to compressibility. Huang *et al.*⁵ use channel flow data at Mach 1.5 and 3.0 to compute the budget of these source terms. They present detailed analysis of the compressibility terms and develop models for them. Similar results are presented by Guarini *et al.*⁶ for a Mach 2.5 boundary layer. However, in contrast to incompressible flows, there is no comprehensive testing of the models for all the source terms in the k -equation.

The usual approach for computing the dissipation rate in a compressible flow is to solve a modeled transport equation for the solenoidal part, ϵ_s , and model the dilatational part, ϵ_d , in terms of the former. It is assumed that ϵ_s follows the same dynamics as ϵ in an incompressible flow, and therefore the modeled ϵ -equation for incompressible flows is used for computing ϵ_s . This approach is universally accepted, however there is very little understanding of the underlying assumption. Specifically, there is no rigorous study of how the exact form of the transport equation for ϵ_s relates to the incompressible ϵ -equation. k and ϵ are computed from the modeled transport equations and then used to compute the Reynolds stresses. The low Re damping functions developed for incompressible flows are used in the compressible case. Once again, there has been no evaluation of these damping functions against compressible DNS data. To summarize,

more research is required to test the $k - \epsilon$ model for its use in compressible flows. Evaluating the model against DNS data will lead to better understanding of its limitations so that it can be improved to predict compressible turbulent flows more reliably.

In this paper, we assess the accuracy of the $k - \epsilon$ turbulence model using the DNS database of a Mach 4, adiabatic, turbulent boundary layer.⁷ In Section 2, we test different low Re versions of the $k - \epsilon$ model for the Reynolds stress. In Section 3, we present the budget of the turbulent kinetic energy transport equation and evaluate existing models for the source terms against the DNS data. In Section 4, we present a similar budget of the transport equation for the solenoidal dissipation and address its modeling. We study how this equation relates to the incompressible dissipation equation. As pointed out earlier, this is the basis for modeling the ϵ_s -equation. The similarities and the differences between the two equations are pointed out, followed by their modeling implications. Conclusions are presented in Section 5.

2. Reynolds Stress

The Reynolds stress tensor, τ_{ij} , is defined as,

$$\bar{\rho}\tau_{ij} = \overline{\rho u_i'' u_j''} = \bar{\rho} \widetilde{u_i'' u_j''} \quad (1)$$

where the overbar and tilde represent Reynolds and Favre averaging, respectively, u_i'' is the Favre-fluctuating velocity component and ρ is the density. In a zero pressure gradient boundary layer, only $\tau_{xy} = \widetilde{u''v''}$ is important, where u and v are the velocity components in the streamwise, x , and wall normal, y , direc-

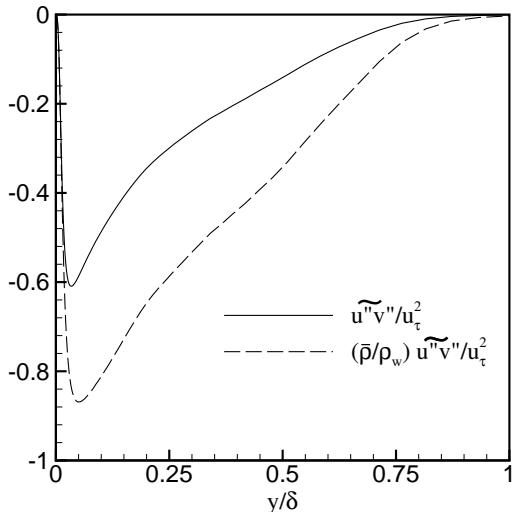


Figure 1. Normalized Reynolds stress in a Mach 4 boundary layer obtained using DNS.

tions. Figure 1 shows the variation of τ_{xy} normalized by u_τ^2 across the boundary layer as computed using the DNS data. u_τ is the friction velocity defined as $\bar{\rho}_w u_\tau^2 = \tau_w$, where $\bar{\rho}_w$ and τ_w are the density and the shear stress at the wall, respectively. Guarini *et al.*⁶ present similar data for a Mach 2.5 boundary layer. They have shown that the normalized Reynolds stress in the compressible flow matches the incompressible data by Spalart⁸ when scaled by the density ratio, $\bar{\rho}/\bar{\rho}_w$. We get similar results using the Mach 4 boundary layer data.

As per the Boussinesq eddy-viscosity approximation, $u''v''$ in a zero pressure gradient boundary layer is modeled as

$$-\bar{\rho} \widetilde{u''v''} = \mu_T \frac{\partial \tilde{u}}{\partial y}. \quad (2)$$

The eddy viscosity, μ_T , is modeled in terms of k and ϵ :

$$\mu_T = c_\mu f_\mu \frac{\bar{\rho} k^2}{\epsilon}, \quad (3)$$

where $c_\mu = 0.09$ is a model constant and f_μ is a damping function. $f_\mu = 1$ away from the wall and it is less than 1 close to the wall to account for the effect of viscosity and the damping of turbulence by the solid wall. Different low Re versions of the $k - \epsilon$ turbulence model use different forms of f_μ . Rodi and Mansour² evaluated some commonly used models against DNS data for incompressible channel and boundary layer flows. They compare the model damping functions to an equivalent f_μ computed from the DNS data as follows,

$$f_\mu^{\text{DNS}} = \frac{-\epsilon}{c_\mu k^2} \frac{\widetilde{u''v''}}{\partial \tilde{u}/\partial y}. \quad (4)$$

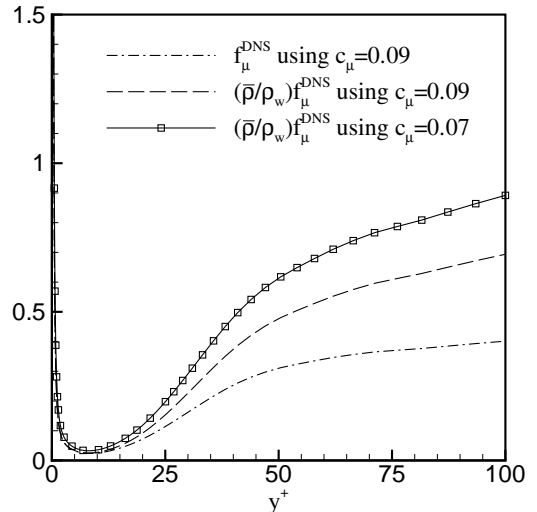


Figure 2. Variation of f_μ^{DNS} with y^+ in a Mach 4 boundary layer.

where Reynolds averaging in Ref. 2 is replaced by Favre averaging for compressible flows. Fig. 2 shows the variation of f_μ^{DNS} with y^+ as computed using DNS data of the Mach 4 boundary layer. Here, $y^+ = yu_\tau/\bar{\nu}_w$ is the non-dimensional distance from the wall, ν is the kinematic viscosity and the subscript w represents the value at the wall. As pointed out earlier, $f_\mu = 1$ away from the wall corresponds to $c_\mu = 0.09$. However, in the boundary layer data in Ref. 2, f_μ^{DNS} attains a value lower than 1 away from the wall ($f_\mu^{\text{DNS}} = 0.83$ at $y^+ = 100$). Thus, the value of c_μ is 0.075 so that $f_\mu^{\text{DNS}} \simeq 1$ away from the wall. In the Mach 4 boundary layer data used here, f_μ^{DNS} attains a value of 0.40 at about $y^+ = 100$. This is much lower than the value reported in Ref. 2 for the incompressible case. However, similar to the Reynolds stress, scaling f_μ with the density ratio improves the comparison with the incompressible damping function. $\tilde{f}_\mu = (\bar{\rho}/\rho_w)f_\mu$ is higher than f_μ (Fig. 2) and is about 0.70 at $y^+ = 100$, which is much closer to the incompressible value. Also, using $c_\mu = 0.07$, instead of the traditional value of 0.09, in the compressible boundary layer we get $\tilde{f}_\mu \simeq 1$ away from the wall.

Next, we compare different low Re $k - \epsilon$ models for the Reynolds stress against the boundary layer data. The damping functions for the models by Launder and Sharma (LS),⁹ Chien (CH),¹⁰ Lam and Bremhorst (LB),¹¹ Shih and Mansour (SM),¹² Nagano and Tagawa (NT),¹³ Rodi and Mansour (RM),² and Myong and Kasagi (MK)¹⁴ are given in Table 1. It is to be noted that some models use a modified dissipation rate, $\tilde{\epsilon}$, in place of ϵ in Eq. (3). $\tilde{\epsilon} = \epsilon - D$, where D for each model is given in Table 1. To facilitate com-

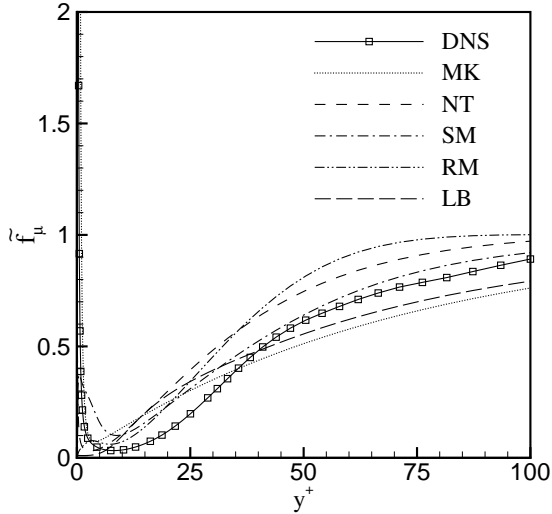


Figure 3. Comparison of model damping functions against \tilde{f}_μ computed from DNS data of a Mach 4 boundary layer. The model codes are given in Table 1.

parison with the DNS data, we compute a modified form of the model damping functions, $\tilde{f}_\mu = f_\mu \epsilon / \tilde{\epsilon}$ and evaluate it against $\tilde{f}_\mu^{\text{DNS}}$ (obtained using $c_\mu = 0.07$). The results are presented in Fig. 3. We see that all the models over-predict the DNS data in the region $y^+ = 10$ through 40, but the final approach of $\tilde{f}_\mu^{\text{DNS}}$ to 1 is better predicted by the model by SM. On the other hand, the models NT and RM approach 1 faster than $\tilde{f}_\mu^{\text{DNS}}$, whereas the models LB and MK approach 1 relatively slow. Some of these models are tested against data for an incompressible boundary layer by Rodi and Mansour² and the comparison shown here is similar to their results. The behavior of the models LS and CH, not shown here, is also similar to the incompressible case. The damping function for LS rises to 1 far too quickly whereas \tilde{f}_μ for CH is much lower than the DNS data and approaches 1 very slowly. Overall, the model by SM is found to be closest to the DNS data.

3. Turbulent Kinetic Energy

In this section, we present a budget of the turbulent kinetic energy computed using the boundary layer data and evaluate models for each source term.

Budget of transport equation

The turbulent kinetic energy in a compressible flow is defined as

$$k = \frac{1}{2} \overline{u_i'' u_i''}, \quad (5)$$

and its transport equation is given by,⁵

$$\frac{D\bar{\rho}k}{Dt} = P_k + T_k + D_k - \bar{\rho}\epsilon + \Pi_k + C_1 + C_2 + C_3. \quad (6)$$

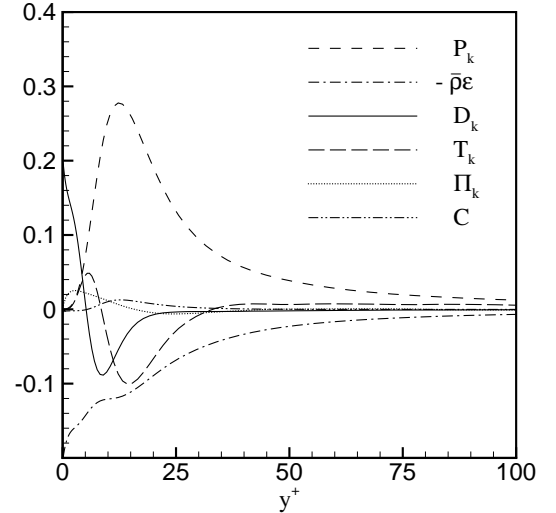


Figure 4. Budget of k -equation using DNS data of a Mach 4 boundary layer. The source terms are normalized by $\bar{\rho}_w u_\tau^4 / \bar{\nu}_w$.

The left-hand side represents the substantial derivative of $\bar{\rho}k$ and it balances the source terms. The first five source terms are turbulent production, turbulent transport, viscous diffusion, viscous dissipation and pressure transport of turbulent kinetic energy, respectively. The last three terms are due to compressibility. The expressions for these source terms are given below,

$$\begin{aligned} P_k &= -\bar{\rho} \overline{u_i'' u_j''} \frac{\partial \tilde{u}_i}{\partial x_j} \\ T_k &= -\left(\overline{\rho u_j'' \frac{1}{2} u_i'' u_i''} \right)_{,j} \\ D_k &= \left(\overline{\sigma'_{ij} u_i''} \right)_{,j} \\ \bar{\rho}\epsilon &= \overline{\sigma'_{ij} u_i''}_{,j} \\ \Pi_k &= -\left(\overline{p' u_i''} \right)_{,i} \\ C_1 &= -\overline{u_i'' \bar{p}}_{,i} \\ C_2 &= \overline{u_i'' \bar{\sigma}}_{,ij} \\ C_3 &= \overline{p' u_i''}_{,i} \end{aligned}$$

where, p is the pressure, σ_{ij} is the viscous stress tensor and the prime represents the Reynolds-fluctuating quantities.

In a zero pressure gradient boundary layer, the unsteady and convection terms on the left-hand side of Eq. (6) are negligible and the turbulent kinetic energy is mainly governed by the source terms. We compute the magnitude of these source terms using the boundary layer data and show the budget in Fig. 4. The source terms are normalized by $\bar{\rho}_w u_\tau^4 / \bar{\nu}_w$. We see

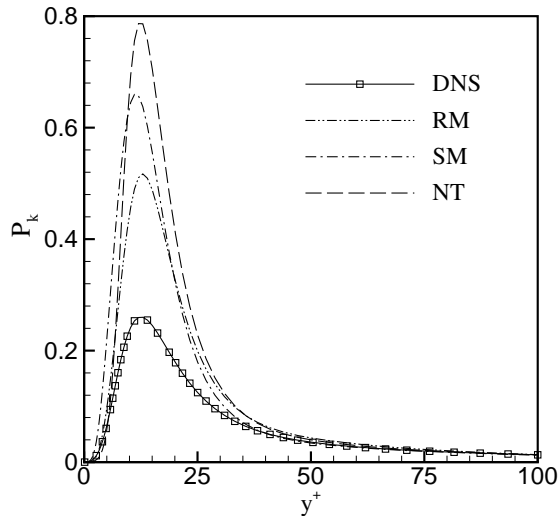


Figure 5. Comparison of models for the production of turbulent kinetic energy, P_k , against DNS data of a Mach 4 boundary layer.

that the budget is very similar to the data presented by Guarini *et al.*⁶ for a Mach 2.5 boundary layer. In the high Reynolds number region, $y^+ > 50$, production, P_k , and dissipation, $\bar{\rho}\epsilon$, are dominant and the other terms are comparatively small. Closer to the wall, production and dissipation are still the largest terms but turbulent transport, T_k , and viscous diffusion, D_k , are also important. The viscous diffusion reaches a maximum at the wall and balances the non-zero dissipation rate. The rest of the terms are zero at the wall. The pressure diffusion term attains a maximum value of 0.025 near the wall and is otherwise small throughout the boundary layer. The sum of the three compressibility terms, C , is also shown. This term has been found to be negligible in a Mach 2.5 boundary layer by Guarini *et al.*⁶ and in Mach 1.5 and Mach 3.0 channel flows by Huang *et al.*⁵ In our boundary layer data at Mach 4, we find that the maximum value of C is 0.013 at about $y^+ = 12$. Also, the magnitude of the compressibility terms C_1 and C_3 are negligible compared to C_2 .

Modeling of source terms

In a boundary layer, the production term simplifies to

$$P_k \simeq -\bar{\rho} \widetilde{u''v''} \frac{\partial \bar{u}}{\partial y}. \quad (7)$$

The modeling of the Reynolds stress, $\widetilde{u''v''}$, in terms of the turbulent eddy viscosity is discussed earlier. We use some of the models for eddy viscosity presented in section 2 to compute P_k and the results are shown in

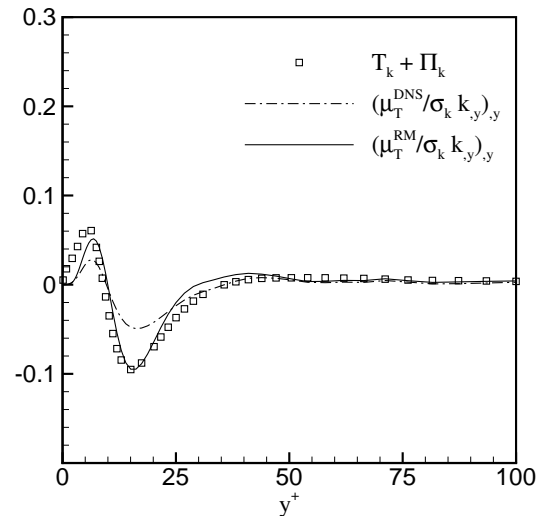


Figure 6. Comparison of models for the turbulent transport, T_k , and pressure transport, Π_k , terms against DNS data of a Mach 4 boundary layer.

Fig. 5 along with the value of P_k as obtained from the DNS data. We see that the models RM and NT reproduce the initial increase in P_k but over-predict the peak value by factors of 2 and 3, respectively. The prediction by SM is in between RM and NT. The remaining models, not shown in Fig. 5, predict even higher values of the peak production. It is to be noted that all the models predict a maximum in P_k at about $y^+ = 10$ which matches the location of the peak in the P_k profile computed from the boundary layer data. Also the models predict P_k in the region $y^+ > 40$ fairly well.

Next, we consider the turbulent transport, T_k , and pressure transport, Π_k , terms. These two terms are modeled together in terms of the turbulent viscosity and the gradient of the turbulent kinetic energy,

$$T_k + \Pi_k \simeq \frac{\partial}{\partial y} \left(\frac{\mu_T}{\sigma_k} \frac{\partial k}{\partial y} \right). \quad (8)$$

Here, $\sigma_k = 1.3$ is the Prandtl number corresponding to the turbulent diffusion of k . To check the validity of the gradient transport assumption, we first compute μ_T using DNS data for $\widetilde{u''v''}$ and $\partial \bar{u} / \partial y$ in Eq. (2). Using this value of the eddy viscosity, denoted by μ_T^{DNS} , we can eliminate the errors due to modeling of μ_T . We see that $(\mu_T^{\text{DNS}} k_y)_y / \sigma_k$ reproduces the variation in $T_k + \Pi_k$ with y but under-predicts the magnitude of the peaks (Fig. 6). Mansour *et al.*¹⁵ show similar comparison between the model and the source term in an incompressible channel flow. This may be due to too high a value of σ_k . Next, we compute μ_T using the turbulence models discussed earlier. We

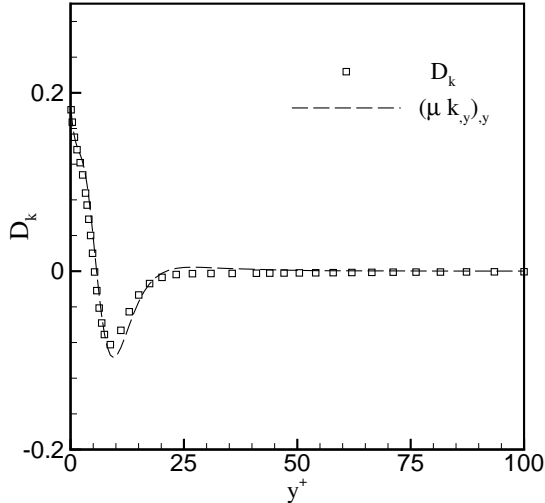


Figure 7. Comparison of the gradient transport model for the viscous diffusion term, D_k , against DNS data of a Mach 4 boundary layer.

have seen in Fig. 2 that the models over-predict the value of μ_T in the range $y^+ < 25$. These modeled values of μ_T result in a higher value of the peaks of the model expression in Eq. (8), which match $T_k + \Pi_k$ better than μ_T^{DNS} . The model by RM is closest to the DNS data, whereas other models over-predict the magnitude of $T_k + \Pi_k$. The viscous diffusion term, D_k , is modeled in a manner similar to the turbulent transport term using the gradient transport hypothesis. Huang *et al.*⁵ have presented a detailed analysis of this term to show that

$$D_k \simeq \frac{\partial}{\partial y} \left(\bar{\mu} \frac{\partial k}{\partial y} \right), \quad (9)$$

where $\bar{\mu}$ is the mean molecular viscosity of the fluid. We see that the above equation is approximately true for this test case (Fig. 7).

The dissipation rate, ϵ , of the turbulent kinetic energy can be split into the solenoidal part, ϵ_s , the dilatational part, ϵ_d , the anisotropy part and additional terms due to fluctuations in the molecular viscosity.⁵

$$\begin{aligned} \bar{\rho} \epsilon_s &= \bar{\mu} \overline{\omega'_i \omega'_i} \quad \text{with} \quad \omega = \nabla \times \mathbf{u}, \\ \bar{\rho} \epsilon_d &= \frac{4}{3} \bar{\mu} \overline{u'_{i,i} u'_{k,k}}, \end{aligned} \quad (10)$$

where, ω is the vorticity. Fig. 8 shows the variation of the total dissipation, the solenoidal dissipation and the dilatational dissipation in the boundary layer. All the quantities are normalized by u_τ^4/ν_w . We see that $\epsilon_d \ll \epsilon_s$ which is similar to the results obtained by Huang *et al.*⁵ for the channel flows with cooled walls and for a boundary layer on adiabatic wall by Guarini

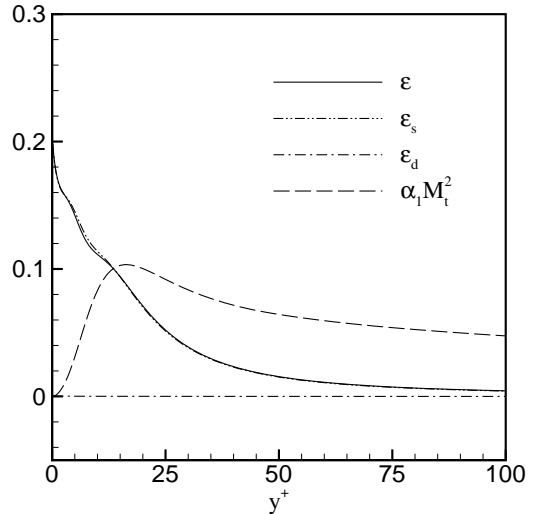


Figure 8. Total dissipation rate, ϵ , and its solenoidal, ϵ_s , and dilatational, ϵ_d , parts as computed using DNS data of a Mach 4 boundary layer. All the dissipation rates are normalized by u_τ^4/ν_w . $\alpha_1 M_t^2$ is also presented for comparison.

*et al.*⁶ The ratio, ϵ_d/ϵ_s is less than 3% throughout the boundary layer. Huang *et al.* have also reported that ϵ_s/ϵ is as low as 0.8 in the viscous sub-layer. This is largely due to the fact that correlation between the viscosity fluctuations and the velocity gradient contributes to the total dissipation. However, in our adiabatic boundary layer, we find that $\epsilon_s/\epsilon \simeq 1$ (Fig. 8).

The solenoidal dissipation-rate is computed from a modeled transport equation which is discussed in detail in the next section. The dilatational dissipation is modeled in terms of ϵ_s as

$$\epsilon_d = \alpha_1 M_t^2 \epsilon_s, \quad (11)$$

where $M_t = \sqrt{2k}/\tilde{a}$ is the turbulent Mach number, \tilde{a} is the Favre-averaged speed of sound and $\alpha_1 = 1.0$ is the generally accepted model constant. We see that $\alpha_1 M_t^2$, as computed using the DNS data, is much larger than ϵ_d/ϵ_s . Thus, the above model greatly over-predicts the dilatational dissipation. This is similar to the observations in other compressible flows.^{5,6}

The compressible source terms C_1 and C_2 involve $\overline{u''_i}$ which needs to be modeled. The values of the stream-wise, $\overline{u''}$, the wall normal, $\overline{v''}$, and the span-wise, $\overline{w''}$, fluctuations normalized by the edge velocity, U_e , are presented in Fig. 9. We see that $\overline{u''}$ is the largest of the three components and attains a peak value of about 15% of the edge velocity. The wall-normal component is about 2% of U_e , whereas the span-wise component is almost negligible throughout

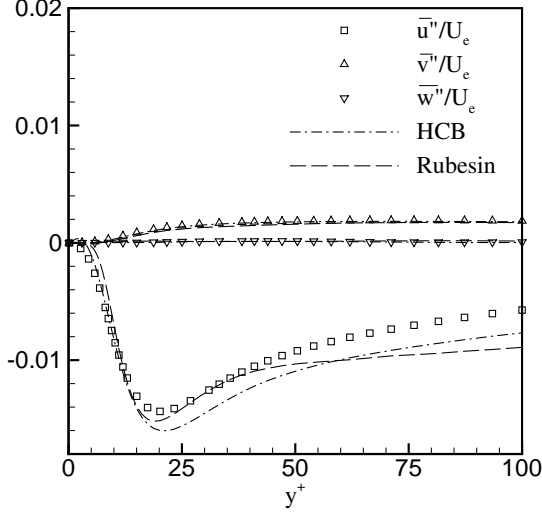


Figure 9. Comparison of models for $\overline{u''}$, $\overline{v''}$ and $\overline{w''}$ against DNS data of a Mach 4 boundary layer. The two models are HCB by Huang *et al.*⁵ and Rubesin.¹⁶

the boundary layer. Huang *et al.*⁵ proposed the following model for u_i'' ,

$$\overline{u_i''} = \frac{1}{\tilde{T}} \frac{u_i'' \tilde{T}''}{u_i'' v_i''} \widetilde{u_i''}, \quad (12)$$

where T is the temperature. The model is based on compressible channel flow data where the pressure fluctuations are negligible compared to the density and temperature fluctuations (Coleman *et al.*¹⁷). In the Mach 4 boundary layer data used in this paper, the pressure fluctuations are found to be small and thus the above model is expected to do well for this test case. Comparing the model against the DNS data in Fig. 9, we see that the predictions for $\overline{v''}$ and $\overline{w''}$ are very good whereas $\overline{u''}$ is marginally over-predicted. The $\overline{u_i''}$ -model proposed by Rubesin¹⁶ is given by

$$\overline{u_i''} = -c_i \frac{k}{\epsilon} \frac{u_i'' \widetilde{v''}}{\epsilon} \frac{\partial \tilde{T}}{\partial y} \frac{1}{\tilde{T}}, \quad (13)$$

where c_i is a calibration constant and \tilde{T} is the Favre-averaged temperature. A value of $c_1 = 0.7$ reproduces the peak in $\overline{u''}$ well but over-predicts the values in rest of the boundary layer, whereas $c_2 = 0.1$ reproduces $\overline{v''}$ very well in almost all of the boundary layer.

4. Solenoidal Dissipation Rate

$k - \epsilon$ modeling of compressible flows solve a modeled transport equation for the solenoidal dissipation. Here, we start with the exact form of the ϵ_s -equation

followed by the budget as computed using the boundary layer data. The modeled ϵ_s -equation is a direct extension of the incompressible dissipation equation. We compare these two equations to assess the accuracy of this modeling approach.

Budget of transport equation

The solenoidal dissipation rate, ϵ_s , is given by

$$\epsilon_s = \bar{\nu} \left(\overline{u'_{i,j} u'_{i,j}} - \overline{u'_{i,j} u'_{j,i}} \right), \quad (14)$$

where $\bar{\nu}$ is the mean kinematic viscosity. The transport equation for ϵ_s has the following form

$$\frac{D\epsilon_s}{Dt} = P_\epsilon^1 + P_\epsilon^2 + P_\epsilon^3 + P_\epsilon^4 + T_\epsilon + D_\epsilon - Y_\epsilon + T_\epsilon^c + B_\epsilon + C_\epsilon. \quad (15)$$

where the expressions for the various source terms are listed below.

$$\begin{aligned} P_\epsilon^1 &= -\bar{\nu} 2 \overline{(u'_{i,j} - u'_{j,i}) u'_{k,j}} \bar{u}_{i,k} \\ P_\epsilon^2 &= -\bar{\nu} 2 \overline{(u'_{i,j} - u'_{j,i}) u'_{i,k}} \bar{u}_{k,j} \\ P_\epsilon^3 &= -\bar{\nu} 2 \overline{(u'_{i,j} - u'_{j,i}) u'_k} \bar{u}_{i,jk} \\ P_\epsilon^4 &= -\bar{\nu} 2 \overline{(u'_{i,j} - u'_{j,i}) u'_{i,k} u'_{k,j}} \\ T_\epsilon &= -\bar{\nu} \overline{[u'_k (u'_{i,j} - u'_{j,i}) u'_{i,j}]_k} \\ D_\epsilon &= \bar{\nu}^2 \overline{(u'_{i,j} u'_{i,j} - u'_{i,j} u'_{j,i})_{,kk}} \\ Y_\epsilon &= \bar{\nu}^2 2 \overline{(u'_{i,j} - u'_{j,i})_{,k} u'_{i,jk}} \\ T_\epsilon^c &= \bar{\nu} \overline{(u'_{i,j} - u'_{j,i}) u'_{i,j} u'_{k,k}} \\ B_\epsilon &= \bar{\nu} 2 \overline{(u'_{i,j} - u'_{j,i}) \rho_{,j} p_{,i} / \rho^2} \\ C_\epsilon &= \bar{\nu} 2 \overline{(u'_{i,j} - u'_{j,i}) (\nu' u_{i,kk} + \psi_\epsilon)}. \end{aligned}$$

The first four terms represent different production mechanisms. P_ϵ^1 is the mixed production term, P_ϵ^2 is the production by mean velocity gradient, P_ϵ^3 is the gradient production term and P_ϵ^4 represents the turbulent production mechanism. The turbulent transport, viscous diffusion and viscous dissipation of ϵ_s are given by T_ϵ , D_ϵ and Y_ϵ , respectively, whereas the last three terms in Eq. (15) are due to compressibility effects. The compressible transport term, T_ϵ^c , represents the effect of non-zero dilatation, B_ϵ is due to baroclinic torques, and C_ϵ includes the effect of variation in fluid viscosity. ψ_ϵ is given by

$$\begin{aligned} \psi_\epsilon &= \frac{\partial \nu}{\partial x_j} (u_{i,kk} + \frac{1}{3} u_{k,ik}) \\ &+ \frac{\partial}{\partial x_k} \left[-\frac{\mu_{,k}}{\rho} (u_{i,k} + u_{k,i}) + \frac{2\mu_{,i}}{3\rho} u_{k,k} \right]. \end{aligned}$$

A budget of the source terms in Eq. (15) as computed using the DNS data is shown in Fig. 10. Following the work by Rodi and Mansour² for incompressible

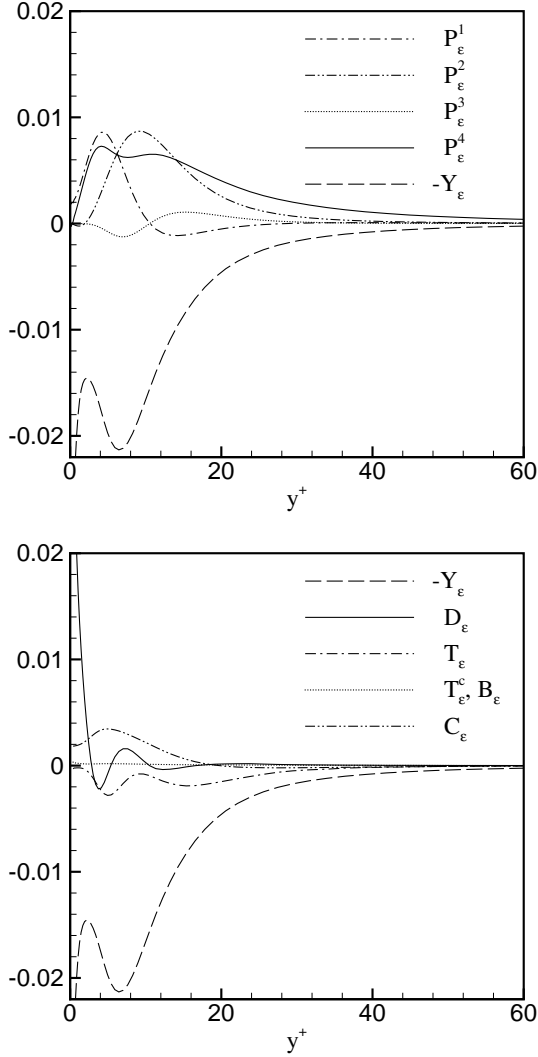


Figure 10. Budget of the ϵ_s -equation computed using DNS data of a Mach 4 boundary layer. All the terms are normalized by $u_\tau^6/\bar{\nu}_w^2$.

flows, we normalize all the source terms by u_τ^6/ν_w^2 . We see that only the turbulent production term, P_ϵ^4 , and the viscous dissipation term, Y_ϵ , are significant in the high Re region away from the wall, and they approximately balance each other. Closer to the wall, P_ϵ^1 and P_ϵ^2 are as large as P_ϵ^4 , whereas P_ϵ^3 is relatively small. This pattern of the production terms is very similar to the data presented by Rodi and Mansour.² The dissipation term is large in this near-wall region to balance all the production terms, whereas the viscous diffusion term, D_ϵ , balances the large negative dissipation at the wall. D_ϵ is small compared to the production terms in the rest of the boundary layer. The magnitude of the turbulent transport term is of the same order as that of the viscous diffusion term, except for very close to the wall. The compressible transport term, T_ϵ^c , and the baroclinic term, B_ϵ , are

negligible, whereas the source term due to variation in fluid viscosity, C_ϵ , is relatively large in the near wall region.

Modeling of transport equation

The modeled transport equation for ϵ_s -equation is not derived from its exact form presented above, rather the modeled dissipation rate equation for incompressible flows is directly used to compute ϵ_s in a compressible flow. This is based on the assumption that ϵ_s follows the same dynamics as ϵ_i in an incompressible flow. (Here, the subscript i is used to represent the incompressible flow quantities.) In other words, it is assumed that the transport equations for ϵ_s and ϵ_i have the same form. Here, we check the validity of this assumption by comparing the exact form of the two equations both analytically and with the aid of the DNS data.

The dissipation rate in an incompressible flow is defined as²

$$\epsilon_i = \nu \overline{u'_{i,j}u'_{j,i}}, \quad (16)$$

and the transport equation for ϵ_i is given by

$$\frac{D\epsilon_i}{Dt} = P_i^1 + P_i^2 + P_i^3 + P_i^4 + T_i + \Pi_i + D_i - Y_i, \quad (17)$$

where

$$\begin{aligned} P_i^1 &= -\nu 2 \overline{u'_{i,j}u'_{k,j}} \bar{u}_{i,k}, \\ P_i^2 &= -\nu 2 \overline{u'_{i,j}u'_{i,k}} \bar{u}_{k,j}, \\ P_i^3 &= -\nu 2 \overline{u'_{i,j}u'_k} \bar{u}_{i,jk}, \\ P_i^4 &= -\nu 2 \overline{u'_{i,j}u'_{i,k}u'_{k,j}}, \\ T_i &= -\nu \overline{[u'_k u'_{i,j} u'_{i,j}]_{,k}}, \\ \Pi_i &= -\nu 2 \overline{[u'_{i,j} p'_{,j}]_{,i}} / \rho, \\ D_i &= \nu^2 \overline{(u'_{i,j} u'_{i,j})_{,kk}}, \\ Y_i &= \nu^2 2 \overline{u'_{i,jk} u'_{i,jk}}. \end{aligned}$$

Once again, the subscript i distinguishes the source terms in the incompressible case from those in the compressible equation (15). The nomenclature of the terms is the same as that in the ϵ_s -equation. P_i^1 , P_i^2 , P_i^3 and P_i^4 represent the mixed production, the production due to mean velocity gradient, the gradient production term and the turbulent production mechanism, respectively. The remaining terms, T_i , Π_i , D_i and Y_i , represent turbulent transport, pressure transport, viscous diffusion and viscous dissipation, respectively. Comparing the ϵ_s -equation with Eq. (17), we see that the four production terms, the turbulent transport term, the viscous diffusion term and the viscous dissipation term are present in both the equations. These are referred as the common terms hereafter. However, there are additional terms — namely,

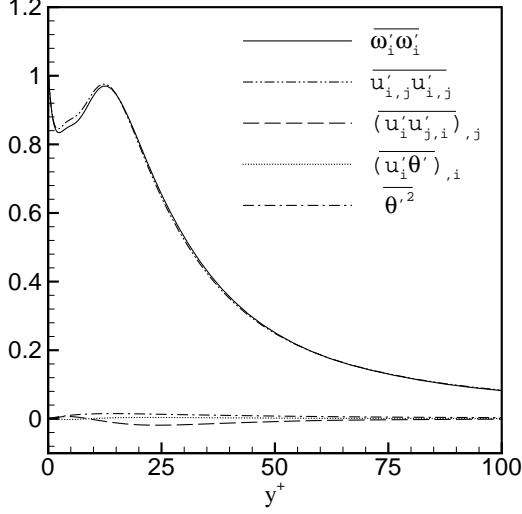


Figure 11. Comparison of the terms in Eq. (18) as computed using the Mach 4 boundary layer data. All the quantities are normalized by $(\overline{\omega'_i \omega'_i})_w$.

Π_i in the incompressible equation and the compressible terms in the ϵ_s -equation. To check whether ϵ_s follows the same dynamics as ϵ_i , we compare the expressions for ϵ_s and ϵ_i . We then compare their transport equations – first, the common terms, and then the extra terms.

The solenoidal dissipation rate in Eq. (14) can be written as $\epsilon_s = \bar{\nu} \overline{\omega'_i \omega'_i}$, where

$$\begin{aligned} \overline{\omega'_i \omega'_i} &= \overline{u'_{i,j} u'_{i,j}} - \overline{u'_{i,j} u'_{j,i}} \\ &= \overline{u'_{i,j} u'_{i,j}} - \frac{\partial}{\partial x_j} \overline{u'_i u'_{j,i}} - \frac{\partial}{\partial x_i} \overline{u'_i \theta'} + \overline{\theta'^2}. \end{aligned} \quad (18)$$

Here, $\theta' = u'_{j,j}$ is the fluctuating dilatation. The last three terms represent the effect of inhomogeneity, the velocity-dilatation correlation and compressibility, respectively. Fig. 11 shows the magnitude of the terms in the above equation in the boundary layer. As noted earlier, $\theta'^2 \ll \overline{\omega'_i \omega'_i}$. We also see that the second and the third terms in (18) have negligible contribution to the enstrophy. The last three terms constitute $\overline{u'_{j,i} u'_{i,j}}$, and therefore

$$\overline{u'_{j,i} u'_{i,j}} \ll \overline{u'_{i,j} u'_{i,j}}. \quad (19)$$

Thus, ϵ_s can be seen as composed of two terms, the first is identical to ϵ_i and the second part represents the effect of inhomogeneity and compressibility. As seen above, the second term is negligible compared to the first, and therefore

$$\epsilon_s \simeq \bar{\nu} \overline{u'_{i,j} u'_{i,j}}. \quad (20)$$

Thus, ϵ_s is equivalent to ϵ_i in a compressible flow.

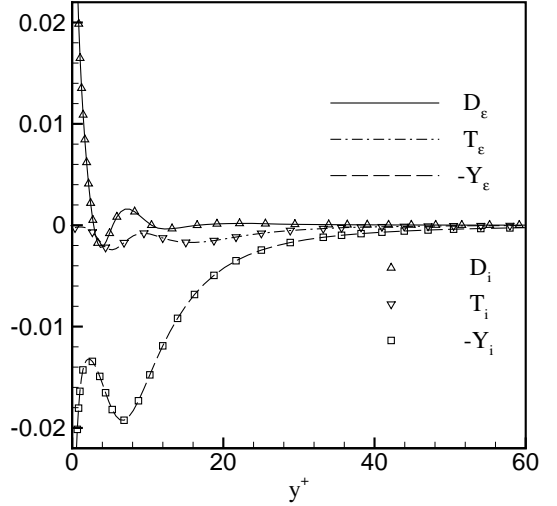
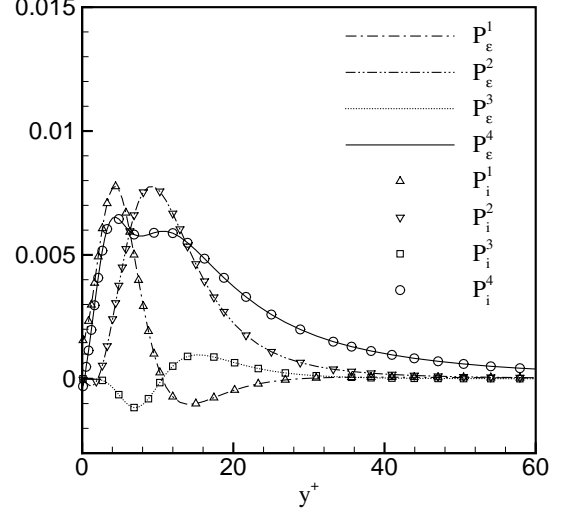


Figure 12. Source terms in the ϵ_s -equation along with the corresponding incompressible terms (symbols) given in Eq. (21) as computed using the DNS data.

Next, we extend the above analysis for ϵ_s to the common source terms in the transport equation (15) which have a corresponding term in the ϵ_i -equation. Each source term is split into two parts – the first part is identical to the respective incompressible source term and the second part represents the effect of inhomogeneity and compressibility.

$$P_\epsilon^1 = P_i^1 + 2 \bar{\nu} \overline{u'_{j,i} u'_{k,j}} \bar{u}_{i,k}$$

$$P_\epsilon^2 = P_i^2 + 2 \bar{\nu} \overline{u'_{j,i} u'_{i,k}} \bar{u}_{k,j}$$

$$P_\epsilon^3 = P_i^3 + 2 \bar{\nu} \overline{u'_{j,i} u'_{i,k}} \bar{u}_{i,jk}$$

$$P_\epsilon^4 = P_i^4 + 2 \bar{\nu} \overline{u'_{j,i} u'_{i,k} u'_{k,j}}$$

$$T_\epsilon = T_i + \bar{\nu} \overline{[u'_{k,i} u'_{j,i} u'_{i,j}]_{,k}}$$

$$D_\epsilon = D_i - \bar{v}^2 \left(\overline{u'_{i,j} u'_{j,i}} \right)_{,kk}$$

$$Y_\epsilon = Y_i - 2 \bar{v}^2 \overline{u'_{j,ik} u'_{i,jk}} \quad (21)$$

We compute the above terms using the boundary layer data and find that the second part of each source term is negligible compared to the first part. This is analogous to the result presented in Eq. (19). Fig. 12 shows this result where each of the above source terms is identical to its respective first part. Thus, the transport equation for solenoidal dissipation simplifies to

$$\frac{D\epsilon_s}{Dt} = P_i^1 + P_i^2 + P_i^3 + P_i^4 + T_i + D_i - Y_i + C_\epsilon. \quad (22)$$

In the above equation, we have neglected the compressible transport term, T_ϵ^c , and the baroclinic term, B_ϵ , which are shown to be negligible in Fig. 10. Comparing the simplified ϵ_s -equation (22) with the incompressible dissipation equation (17), we see that the two equations are identical except for the terms Π_i and C_ϵ . The pressure transport term, Π_i , in the incompressible equation is found to be negligible by Rodi and Mansour,² whereas the effect of the viscosity variation term, C_ϵ , is not negligible (Fig. 10) and should be accounted for. The incompressible models for the rest of the source terms can be extended to the compressible case.

5. Conclusions

We evaluate the $k - \epsilon$ turbulence model using DNS data of a Mach 4 boundary layer. The results are presented in three parts. First, the low Re models for the Reynolds stress are tested. We find that the models must be corrected by the density ratio to match the DNS data. Next, we present the budget of the k equation and test models for each source term. The models predict too high a peak for the production term, whereas the models for the turbulent transport, pressure transport, viscous diffusion and the compressible terms perform reasonably well. The dilatational dissipation is negligible compared to the solenoidal part, but the model grossly over-predicts its value. We compute the budget of the solenoidal dissipation rate, ϵ_s , and find it to be similar to the budget of the dissipation rate, ϵ_i , in an incompressible flow.² The modeling of the ϵ_s equation is based on its equivalence to the ϵ_i equation. Comparison of the two equations, analytically and with the aid of DNS data, shows that they are identical except for a source term due to the variation of fluid viscosity in the compressible case. Thus, the modeled incompressible dissipation rate equation can be used to compute ϵ_s , but the effect of the additional term must be included.

Acknowledgments

We would like to acknowledge the support from the Air Force Office of Scientific Research Grant number No. AF/F49620-98-1-0035. This work was also sponsored by the Army High Performance Computing Research Center under the auspices of the Department of the Army, Army Research Laboratory cooperative agreement number DAAH04-95-2-0003 / contract number DAAH04-95-C-0008, the content of which does not necessarily reflect the position or the policy of the government, and no official endorsement should be inferred. A portion of the computer time was provided by the University of Minnesota Supercomputing Institute.

References

- ¹ Mansour, N.N., Kim, J., and Moin, P., "Reynolds-stress and Dissipation-rate Budgets in a Turbulent Channel Flow," *Journal of Fluid Mechanics*, Vol. 194, 1988, pp. 15-44.
- ² Rodi, W., and Mansour, N.N., "Low Reynolds number $k-\epsilon$ Modeling with the aid of Direct Simulation data," *Journal of Fluid Mechanics*, Vol. 250, 1993, pp. 509-529.
- ³ Nagano, Y., and Shimada, M., "Rigorous Modeling of Dissipation-Rate Equation using Direct Simulations," *JSME Int. Journal, Series B*, Vol. 38, No. 1, 1995, pp. 51-59.
- ⁴ Sarkar, S., and So, R.M.C., "A Critical Evaluation of Near-Wall Two-Equation Models against Direct Numerical Simulation Data," *Int. J. Heat and Fluid Flow*, Vol. 18, No. 2, 1997, pp. 197-208.
- ⁵ Huang, P.G., Coleman, G.N., and Bradshaw, P., "Compressible Turbulent Channel flows : DNS results and Modeling," *Journal of Fluid Mechanics*, Vol. 305, 1995, pp. 185-218.
- ⁶ Guarini, S.E., Moser, R.D., Shariff, K., and Wray, A., "Direct Numerical Simulation of a Supersonic Turbulent Boundary Layer at Mach 2.5," *Journal of Fluid Mechanics*, Vol. 414, 2000, pp. 1-33.
- ⁷ Martín, M.P., and Candler, G.V., "DNS of a Mach 4 Boundary Layer with Chemical Reactions," AIAA Paper No. 2000-0399, Jan. 2000. Also in *Recent Advances in DNS and LES*, Kluwer Academic Press, 1999.
- ⁸ Spalart, P.E., "Direct Simulation of a Turbulent Boundary Layer up to $Re_\theta = 1410$," *Journal of Fluid Mechanics*, Vol. 187, 1988, pp. 61-98.

- ⁹ Launder, B.E., and Sharma, B.I., "Application of the Energy Dissipation Model of Turbulence to the Calculation of Flow near a Spinning Disc," *Lett. Heat Mass Transfer*, Vol. 1, No. 2, 1974, pp. 131-138.
- ¹⁰ Chien, K.Y., "Prediction of Channel and Boundary-Layer flows with a Low-Reynolds-Number turbulence model," *AIAA Journal*, Vol. 20, No. 1, 1982, pp. 33-38.
- ¹¹ Lam, C.K.G., and Bremhorst, K.A., "Modified Form of the $k - \epsilon$ Model for Predicting Wall Turbulence," *Journal of Fluid Engineering*, Vol. 103, 1981, pp. 456-460.
- ¹² Shih, T-H, and Mansour, N.N., "Modeling of Near Wall Turbulence," In *Engineering Turbulence Modeling and Experiments*, (ed. W. Rodi and E.N. Ganic), Elsevier, 1990, pp. 13-19.
- ¹³ Nagano, Y., and Tagawa, M., "An Improved $k - \epsilon$ Model for Boundary Layer Flows," *Journal of Fluids Engineering*, Vol. 112, 1990, pp. 33-39.
- ¹⁴ Myong, H.K., and Kasagi, N., "A New Approach to the Improvement of $k - \epsilon$ Turbulence Model for Wall-Bounded Shear Flows," *JSME International Journal*, Vol. 33, 1990, pp. 63-72.
- ¹⁵ Mansour, N.N., Kim, J., and Moin, P., "Near-Wall $k - \epsilon$ Turbulence Modeling," *AIAA Journal*, Vol. 27, No. 8, 1989, pp. 1068-1073.
- ¹⁶ Rubesin, M.W., "Extra Compressibility Terms for Favre-Averaged Two-Equation Models of Inhomogeneous Turbulent Flows," NASA CR-177556, 1990.
- ¹⁷ Coleman, G.N., Kim, J., and Moser, R.D., "A Numerical Study of Turbulent Supersonic Isothermal-wall Channel Flow," *Journal of Fluid Mechanics*, Vol. 305, 1995, pp. 159-183.